Received: 10 November 2022 | Revised: 18 April 2023 | Accepted: 20 April 2023

DOI: 10.1002/hyp.14890

RESEARCH ARTICLE

WILEY

Groundwater flow reversal between small water bodies and their adjoining aquifers: A numerical experiment

Jörg Steidl[1] | Steffen Gliege[1,2] | Majid Taie Semiromi[1] | Gunnar Lischeid[1,3]

[1]Leibniz Centre for Agricultural Landscape Research (ZALF), Institute of Landscape Hydrology, Müncheberg, Germany

[2]Freie Universität Berlin, Institute of Geological Sciences, Hydrogeology Group, Berlin, Germany

[3]Institute of Environmental Science and Geography, University of Potsdam, Potsdam, Germany

Correspondence
Jörg Steidl, Leibniz Centre for Agricultural Landscape Research (ZALF), Institute of Landscape Hydrology, Eberswalder Str. 84, 15374 Müncheberg, Germany.
Email: jsteidl@zalf.de

Abstract

The countless kettle holes in the Late Pleistocene landscapes of Northern Europe are hotspots for biodiversity and biogeochemical processes. As a rule, they are hydraulically connected to the shallow groundwater system. The rapid, intensive turnover of carbon, nutrients and pollutants in the kettle holes therefore has a major impact on the quality of the shallow groundwater downstream. As a result of high-evapotranspiration rates from their riparian vegetation or strong storm events, the process of downstream groundwater flow may stagnate and reverse back towards the kettle hole, making interactions between the groundwater and kettle hole more complex. Furthermore, the highly heterogeneous soil landscape in the catchment contributes to this complexity. Therefore, the present study aims to enhance our understanding of this complicated interaction. To this end, 24 model variants were integrated into HydroGeoSphere, capturing a wide range of uncertainties in quantifying the extent and timing of groundwater flow reversal between a kettle hole and the adjacent aquifer. The findings revealed that the groundwater flow reversal lasted between 1 month and 19 years at most and occurred in a distance of more than 140 m downstream of the kettle hole. Our results demonstrated that the groundwater flow reversal arises especially often in areas where the shallow aquifer possesses low-hydraulic conductivity. There may also be a recurrent circulating flow between the groundwater and kettle hole, resulting in solute turnover within the kettle hole. This holds particularly true in dry periods with medium to low-water levels within the kettle hole and a negative water balance. However, shallow groundwater flow reversals are not necessarily a consequence of seasonal effects. In this respect, the properties of the local shallow aquifer by far outweigh the effect of the kettle hole location in the regional flow regime.

KEYWORDS

groundwater flow reversal, HydroGeoSphere, kettle hole, numerical experiment, surface–groundwater interaction

1 | INTRODUCTION

Surface waters and groundwater bodies are closely related. Nevertheless, they have often been studied separately in different environmental disciplines (Akbari et al., 2022; Bailey et al., 2016; Winter, 1999; Winter, 2001). Under certain circumstances they are treated as a single entity or the interface between the two and the exchange of water and solute is simplified (Taie Semiromi and Koch, 2019). For example, the

exchange flow between a groundwater domain and lake is assumed to be stable where the groundwater aquifer is constantly replenished by the lake inflow. In reality, however, the lake–groundwater interactions are highly dynamic in time and space (Bailey et al., 2016). This common approach can be particularly problematic for landscapes where the terrain is spotted with thousands of water-filled glaciogenic depressions known as kettle holes.

Kettle holes are postglacial landscape features typical of the young Pleistocene moraine areas in Northern Europe and Northern America. The term "kettle holes" is used by preference in Europe (Kalettka & Rudat, 2006; Schweizer, 2012), while "potholes" is a synonym in Northern America (Mitsch & Gosselink, 2015). In the northeast of Germany, kettle holes are estimated to range in number from 150 000 to 300 000, broadly populating an area of 38 000 km^2. Kettle holes are distinguished from lakes by their smaller water surface area of up to one hectare, making them more prone to falling dry. Kettle holes have a high informative value. Their hydrological function is viewed as a suitable indicator not only for assessing of the changes related to the regionally connected hydrological system (Amado et al., 2018; Hayashi et al., 2016) but also for tracing water and matter through the hydrologic cycle. In comparison with larger water bodies, kettle holes receive substantially larger inputs of pesticides (Lorenz et al., 2017), plant biomass, soil particles via erosion, and nutrients (e.g., fertilizers) (Nitzsche et al., 2017) due to their close connection to adjacent agricultural fields, in combination with their intrinsically shallow water system. Therefore, the particular importance of kettle hole/pothole hydrology is in understanding the processes influencing the quality and quantity of individual water components in the water balance equation, how they interact, and how they react to climatic variability and land-management practices (Nitzsche et al., 2017).

In this context, the kettle holes memory effect, their role in soil moisture enhancement (Hayashi et al., 2003; Logan & Rudolph, 1997), and their focused groundwater recharge (Berthold et al., 2004) are regarded as important hydrological functions, while their maintenance of regional biodiversity and stability is considered an important ecological function (Downing, 2010). Thus, kettle holes play a crucial role as hotspots for biodiversity (Pätzig et al., 2012), material accumulation (Kalettka et al., 2001; Kazmierczak, 1997), biogeochemical transformations (Lischeid & Kalettka, 2012) and chemical leaching into shallow groundwater (Derby & Knighton, 2001; Hayashi et al., 2003; Parsons et al., 2004; Stumpp & Hendry, 2012).

Kettle holes are often surrounded by uplands and appear to be isolated from each other or even from nearby streams in terms of water exchange (Cohen et al., 2016; Leibowitz, 2015). Nonetheless, the term "isolated" has been criticized as a misnomer (Leibowitz, 2015; Mushet et al., 2015) because physiographically isolated kettle holes can receive groundwater inflows from shallow groundwater flow systems that extend well beyond their surface watershed (Winter et al., 2003). This is the only possible type of almost continuous hydrological connection between kettle holes of different areas that drain internally without appreciable surface runoff (Neff & Rosenberry, 2018), as it is the case in the Uckermark region, located in the northeast of Brandenburg, Germany (Lischeid et al., 2018).

The Kettle holes' effect on the water quality is dependent on the concentrations and loads received from the groundwater, as well as the water residence time in the kettle holes, which is important for the kinetics of the substance transformation processes. In that regard, groundwater that has already flowed through a kettle hole is of a different quality from the water that enters the kettle hole on the upstream side. These effects need to be considered quantitatively when investigating biogeochemical processes in a kettle hole. In that regard, Hayashi et al. (1998) investigated the water and solute transfer between a pothole and the adjacent shallow aquifer. The interaction between potholes and their shallow groundwater domains is described by van der Kamp and Hayashi (2009) and analysed by Heagle et al. (2013) and Ferone and Devito (2004). In addition, kettle holes can be regarded as windows posing a high risk of contamination to groundwater. This especially holds true for regions in which multiple kettle holes are often located along the same groundwater flow line (Lischeid et al., 2016), meaning that cumulative effects have to be considered.

Different situations can lead to the downstream flow of the adjoining shallow groundwater to reverse back to a kettle hole. For instance, high evapotranspiration via plants (i.e., reeds, bulrushes, etc.) in the encircling vegetation belt (Winter, 1999; Xu & Ma, 2011) may reverse the groundwater flow as explored by several studies (e.g., Ferone & Devito, 2004, Gerke et al., 2010, Heagle et al., 2013, van der Kamp and Hayashi, 2009). Moreover, heavy storms or wet periods can result in groundwater mounding, reversing the flow from the groundwater towards the kettle hole. Although this phenomenon is well known for larger water bodies such as lakes, bogs, and so forth. (e.g., Anderson & Munter, 1981; Devito et al., 1997; Fraser et al., 2001; Winter, 1999), it has been poorly documented for kettle holes to date. In these conditions, understanding the hydraulic head dynamics in both the groundwater and kettle hole becomes much more complex. Gerke et al. (2010) described the importance of the colluvial fringe of kettle holes as a sensitive area for lateral exchange fluxes and pointed out the limitations induced by the unknown complexity of relevant soil hydraulic properties and sediment structures. This kind of complexity due to erosion processes sometimes has also affected the areas where groundwater is recharged. When the unsaturated zone varies in thickness due to the surface relief, this can cause the groundwater recharge to be completely different in terms of time and quantity even under very similar soils. However, this is not the only complexity that causes problems when modelling flows to or from groundwater (Groh et al., 2020).

As the findings of field studies are difficult to generalize, in particular for larger surface waters such as lakes, several analytical, steady-state, transient and often hypothetical modelling approaches were developed in the past to classify possible flow regimes (Anderson & Munter, 1981; Townley & Davidson, 1988; Winter, 1976; Winter, 1983; Zheng et al., 1988).

Since then, attention has also been paid to the simulation of the water balance and subsurface interconnection among kettle holes (e.g., Liu et al., 2016, Amado et al., 2018, Vyse et al., 2020). The flow regime and the mixing between the kettle hole and groundwater can be simulated in a significantly more reliable manner if the

hydrologically relevant properties of a landscape can be considered using plausible parameters included in different model variants covering a wide range of uncertainty.

Along with other hydrological models, recent studies have employed the state-of-the-art, fully integrated hydrological model HydroGeoSphere (HGS) (Aquanty, 2013) to quantify the pothole/kettle hole–groundwater exchange. Golden et al. (2014) and Amado et al. (2018) assert, for instance, that HGS could provide a useful insight into the key hydrological processes involved in the land surface and the unsaturated and saturated domain, which control the hydrologic connectivity between potholes and the proximate shallow groundwater system.

As kettle holes are expected to have a significant impact on water quality and biogeochemical processes, the overall objective of the present study is to improve our understanding of the flow exchange between the groundwater and kettle hole, enabling us to characterize and quantify the interaction between these two compartments. To do so, we quantify the potential lateral flow exchange between a kettle hole and its adjacent shallow aquifer. In particular, we assess the range and duration of associated groundwater flow reversals between these two compartments. This study is not focused on specific conditions at a single site; rather, it aims to propose a modelling approach for plausibly evaluating the poorly documented process of groundwater flow reversal from an aquifer towards a kettle hole in a very heterogeneous landscape.

2 | MATERIALS AND METHODS

2.1 | Modelling approach

The numerical experiment was performed using the process-based hydrological model HGS mentioned above. The HGS code solves the fully integrated surface and subsurface water flow and solute transport problems in variably saturated media (Therrien et al., 2010). Further, the 2D diffusive-wave equation and the 3D form of the Richards equation are solved simultaneously using a globally implicit approach. Evapotranspiration processes are simulated using the formulation presented in Kristensen and Jensen (1975). Details of the HGS model and the processes and numerical methods implemented can be found in the HGS user manual (Aquanty, 2013).

The particular challenge when implementing the model in the Pleistocene sediments is the known presence of manifold small-scale heterogeneities (Gerke et al., 2010), which cannot be assessed in sufficient detail using available resources because they are usually unknown and often transient.

For this reason, a highly simplified vertical section model from a real geometric situation was implemented here in HGS. The effects of various sources of uncertainty, including the described heterogeneities, were considered by running numerous model variants with different parameterizations and boundary conditions. Consequently, the following properties were varied in a systematic way:

- Lateral boundary condition;
- Hydraulic conductivity and depth of the lower semi-permeable subsurface (aquitard);
- Texture and hydraulic parameters of the shallow aquifer.

Finally, in the case of relevant model variants, a transport boundary condition was added at the bottom of the kettle hole to investigate the transient dispersion of kettle hole water.

2.2 | Study site and spatial discretization

The study site is in the northeast of Brandenburg, Germany. Figure 1 shows the area and position of the kettle hole in question, situated across a flat slope topography between an overlying and an underlying kettle hole; a constellation that is common in this hummocky landscape. In this study, this example serves as a prototype for developing a simplified parsimonious structural model that later form a basis for different hydraulic models with individual parameterizations within the possible range of Pleistocene sediments, including different thicknesses and hydraulic model boundary conditions.

In this respect, data from an intensively studied region in northeastern Brandenburg, Germany, (Kleeberg, Neyen, & Kalettka, 2016), synthesized with regional data following (Merz & Steidl, 2015) and (Premke et al., 2016), were considered to derive reasonable internal geometries and parameter ranges for modelling. For example, as the thickness of the lower semipermeable layer of glacial till significantly exceeds that of the overlying sediments (Merz & Steidl, 2015), a uniform elevation of 80 m a.s.l. was taken as the lower boundary of the model domain (Figure 2). The glacial till is overlaid with a thin layer of silty, sandy and gravelly sediments (Merz & Steidl, 2015), which enable subsurface flow processes to occur between hydraulically connected kettle holes on the one hand and thus the kettle hole and groundwater on the other hand.

The Grid Builder (McLaren, 2008) was used at section A-B (see Figure 1) to transform the terrain surface into a 2D mesh about 1.5 m in width, which is spatially discretized into triangular elements. Between the lower model domain border and this 2D mesh, with terrain elevations as the upper model domain border, nine finite element layers were discretized in a 3D mesh with increasing mesh refinement near the terrain surface (Figure 2). The uppermost nodes match those of the 2D surface mesh. This adjustment was made to improve numerical performance and the quality of the solution at the interface between the upper sediment layer and the atmosphere. Finally, the structural model includes a model area with a length of 402 metres, a width of 1.5 metres and an average thickness of 9.8 metres with a total of 7254 elements and 8080 nodes in a quasi-vertial plane section.

The glacial till represents the lower semipermeable layer (Figure 2). This was specified as clay and was parameterized according to the ROSETTA code (Schaap et al., 2001). ROSETTA uses pedotransfer functions to predict the water retention, the unsaturated hydraulic conductivity parameters and the saturated hydraulic conductivity (K_S) (Van Genuchten, 1980) in a hierarchical manner.

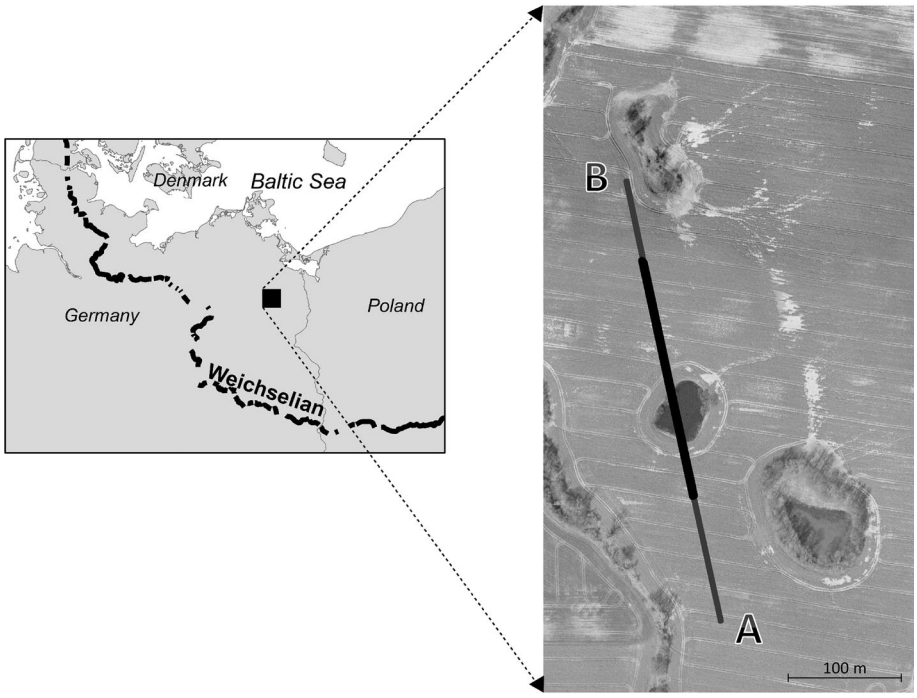

FIGURE 1 The oldest main end moraine (lines) of the Weichselian Pleistocene glaciations with thousands of kettle holes occurring northeast of the divide (left) and the abstracted model section A, B (right) with the main area of interest (black line) and its extensions (grey lines).

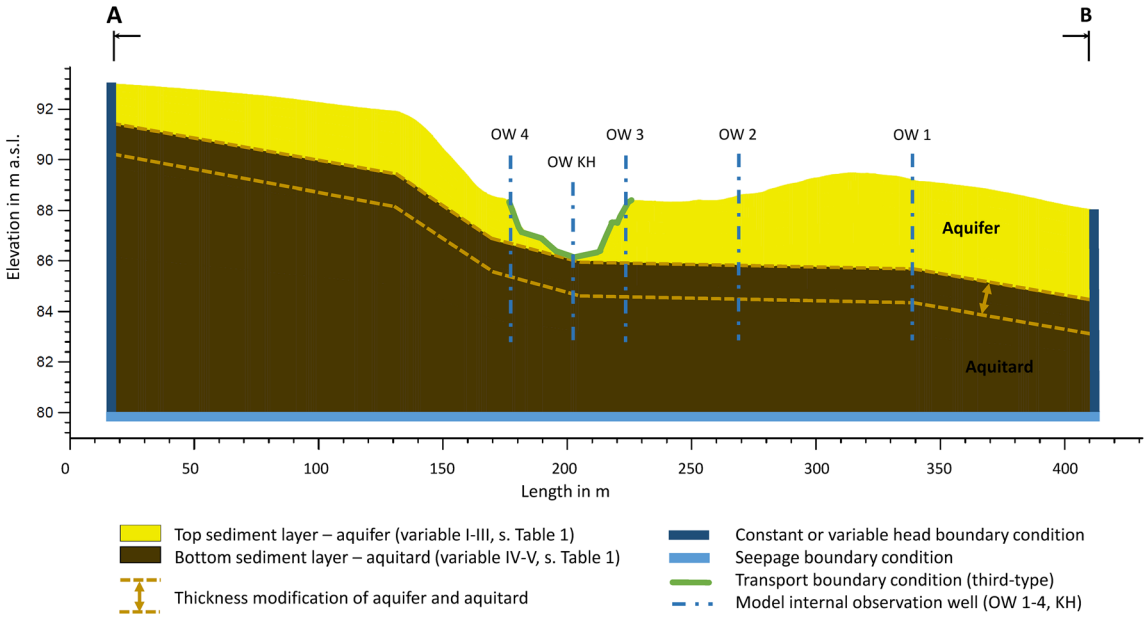

FIGURE 2 Cross section along the vertical plane showing the model domain dimensions of the kettle hole between the adjacent overlying (upstream) and underlying (downstream) kettle holes with sediment layers, boundary conditions and model internal observation wells (A, B see Figure 1). Note different scaling of the x- and y-axes.

Dynamics and variability in agricultural land use were neglected. In this case, the grass cover was defined as homogenous.

2.3 | Model variants

The numeric experiment followed a full factorial design with four factors represented by two or three levels for each factor, resulting in 24 model variants in total. Each model run is characterized by a four-letter code (Table 2).

The first factor was realized by two variants of the lateral boundary conditions. The second factor was varied by the thickness of the top sediment layer, that is, the depth of the interface between the top sediment layer and the glacial till (Figure 2). The third factor was the hydraulic conductivity of the aquitard, which affects the downward leakage flux. For a clear distinction between the two values, we used

the terms "slight" and "weak" to denote a very low and even a much lower hydraulic conductivity, respectively, as compared to those of the top sediment layers. The final factor comprises three variants of the sediment texture of the top layer, which is closely related to the hydraulic properties (Table 1). In all variants, however, the upper confining bed is represented by the sediments of the unconfined aquifer, whereas the underlying glacial till is specified as clay (Figure 2).

In total, 24 model variants were compiled (Table 2), making it possible to characterize and therefore simulate a wide range of possible subsurface conditions.

2.4 | Boundary and initial conditions

Daily precipitation and potential evapotranspiration values for the period from 1 September 1991 to 3 October 2013 were used as the top boundary condition of the model domain. The required data were collected from the meteorological station in Dedelow, near the study site (Verch, 2014). For the area around the kettle hole grass-reference evapotranspiration (Allen et al., 1998) was used as the potential evapotranspiration. Like many other kettle holes, the modelled kettle hole also encompasses very dense shoreline vegetation such as reeds or bulrushes (Figure 1) (Pätzig et al., 2012). Evapotranspiration via emerging hydrophytes can be more than twice as high as the evaporation via the open water surface (Crundwell, 1986; Xu & Ma, 2011). This effect depends on many dynamic factors, such as vegetation density and growth, and can only be considered here by estimating it in the upper model boundary condition. For this reason, the potential evapotranspiration was increased by 60%. Table 3 shows the corresponding evapotranspiration parameters for the homogeneous grass cover both from the ground surface and from the open water surface within the kettle hole.

A seepage boundary condition was applied to the domain bottom to ensure that there was deep seepage throughout the bottom of the model domain. An aquifer underlying the marl is considered to be unconfined and the marl to be thick enough to exclude feedback. The lateral boundaries of the cross section were modelled as specified head boundary conditions. For this purpose, firstly, constant values of

TABLE 3 Evapotranspiration parameters of land and water surface as required by the HGS model

Parameter	Land surface (grass)	Water surface (at kettle hole)
Evaporation depth	1 m	0.1 m
Evaporation depth function	Quadratic decay	Constant
Root zone depth	1 m	0 m
Root depth function	Quadratic decay	Constant
Leaf area index	1	0
Transpiration fitting parameters		
C1	0.4	1
C2	0.1	0
C3	1	1
Transpiration limiting saturations		
Wilting point	0.29	0.2
Field capacity	0.56	0.5
Oxic limit	0.75	1
Anoxic limit	0.9	1
Evaporation limiting saturations		
Minimum	0.2	0.5
Maximum	0.4	0.8
Canopy storage	0 m	0 m
Initial interception storage	0 m	0 m

TABLE 1 Model parameterizations regarding the sediment layers and the corresponding sediment hydraulic properties with K as isotropic, hydraulic conductivity and S_{wr} as residual water saturation

Variable	Layer	Name	$K_{isotropic}$	Porosity	S_{wr}	α	ß
			m d^{-1}	(–)	(–)	m^{-1}	(–)
I	Top	Sand	6.4298	0.3747	0.0530	3.53	3.1798
II	Top	Loamy sand	1.0512	0.3904	0.0485	3.47	1.7466
III	Top	Silty sand	0.9181	0.4086	0.0257	4.48	1.4600
IV	Bottom	Clay	7.80E-05	0.4588	0.0982	1.5	1.2529
V	Bottom	Clay	3.80E-05	0.4588	0.0982	1.5	1.2529

TABLE 2 Four-letter code and designation of the variants of the numeric experiment

Lateral boundary top condition	Vertical position of aquitard	Hydraulic conductivity of aquitard	Texture of layer
s… **s**tatic	.s.. **s**hallow	..w. **w**eak	…S **S**and
d… **d**ynamic	.d.. **d**eep	..s. **s**light	…L **L**oamy sand
			…U Silty sand

91 and 86 m a.s.l. were applied, derived from linear interpolation of the digital elevation model (DTM) values to the extended boundaries. Subsequently, these boundary conditions, in combination with constant precipitation and potential evapotranspiration rates (daily average over the entire period), were used in pre-processing model runs to generate reasonable initial head conditions within the model domain. All required computations, launched with an initial head of 87.7 m a.s.l., were carried out until a steady-state condition was reached. In a second approach, the lateral boundary conditions were specified as a variable head to study a more dynamic behaviour and thus to analyse its influence. To facilitate this, two observation wells, recording the groundwater levels at the outer boundaries of the main section, were used during the model runs with a constant head boundary. By adjusting these data to the level of the extended boundaries, we were able to generate time series of groundwater levels, which were then used as lateral boundary conditions for further investigation. These findings serve in turn as a starting point for the corresponding model applications with a time span from 1 September 1991 to 31 October 2013. At this point, the measured time series of daily values for precipitation and potential evapotranspiration was applied to the top boundary of the model domain. The time period from 1 September 1991 to 31 October 2013 constitutes the entire simulation period. The first three years were seen as a "spin-up" period to adjust the processes until the model reached an "optimal" state (Kim et al., 2018). Therefore, the actual analysis was conducted from 1 November 1994 onwards.

2.5 | Model calibration and evaluation

The hydraulic properties of the subsurface sediments were adapted such that, depending on the model variant, the kettle hole water level just overtoped the banks in wet years, while falling below the kettle hole bed in dry years. This has been observed in various field surveys in that region. Furthermore, corresponding to long-term observations (Lehsten et al., 2011), maximum intra-annual water level fluctuations from around 1.0 m to more than 2.0 m over a period of several years (Heagle et al., 2013) were used as an adjustment criteria. These adaptation criteria were supported by the monitoring data series compiled from the extensive monitoring programme that has been performed in the Quillow catchment since the late 1990s (Merz & Steidl, 2015).

2.6 | Analysing the water origin within the exchange zone

To investigate the spatial extent of the water exchange between the kettle hole and the groundwater domain, we assigned an additional transport boundary condition (mass flux) to nodes covering the kettle hole bed in the model (Figure 2). In this study, a single, non-decaying, conservative solute with a free-solution diffusion coefficient of zero and a specified concentration of 1 mg l^{-1} was used throughout the simulation period to track the propagation of the kettle hole's water to the adjacent shallow aquifer. For other parameters controlling the transport model, the default settings of HGS were used. For longitudinal dispersion this was 1.0 m and for transverse dispersion 0.1 m. As the lateral boundary conditions force a gradient from the higher topography to the kettle hole and from there to the lower topography, the study only considered the portion of the model domain extending from the centre of the kettle hole to the lateral boundary on the downstream side of the kettle hole.

Starting at OW (KH), located at the centre of the kettle hole of interest, and ending 10 m behind OW1 (Figure 2), a line of 30 observation wells spaced at 5 m intervals were integrated into the model domain. Each well recorded the solute concentration at each time step and at 9 different depths, predefined by the discretization of the model domain. Only the water from the kettle hole was injected with a non-reactive and non-decaying solute, meaning that it can be considered as a tracer. As matrix diffusion effects and thermal energy advection were excluded, the mass transfer is determined by the flow. The difference between increasing and decreasing concentrations was used to assess the origin of the water at each time step. For positive values of the first derivative of the concentration and with respect to time, it was thus assumed that the water had originated from the kettle hole. Otherwise, it was assumed that the water originated from the groundwater domain. The respective water sources were aggregated per day for each of the 270 observation wells. These aggregated values were used to determine the spatial extent of the water exchange zone, as well as the location and proportion of the kettle hole water.

3 | RESULTS

3.1 | Kettle hole water level and groundwater head dynamics

The intra-annual variability of the simulated hydrographs was closely related to that of precipitation, which varied between 366 and 761 mm y^{-1} (Figure 3). Similarly, actual evapotranspiration varied between 130 and 562 mm per y^{-1} (Figure 4).

Considering all model variations, the water level of the kettle hole varied between 85.57 and 88.58 m a.s.l. The water level thus fell 0.65 m below the kettle hole bed at 86.22 m a.s.l. and overtopped the banks at 88.37 m a.s.l. by 0.21 m. The variants with pure sand deposits reached the highest water levels (mean 88.15 m a.s.l.), followed by those with loamy sand (87.28 m a.s.l.) and silty sand (86.61 m a.s.l.). The minimum and maximum water levels of the variants with loamy sand were also on average between 0.77 and 1 m below those of the variants with pure sand, and between 1.44 and 1.58 m below those of the variants with silty sand.

The higher water levels in the variants with pure sand can be attributed primarily to the low water storage capacity of the sediment. The comparatively very low evapotranspiration associated with this

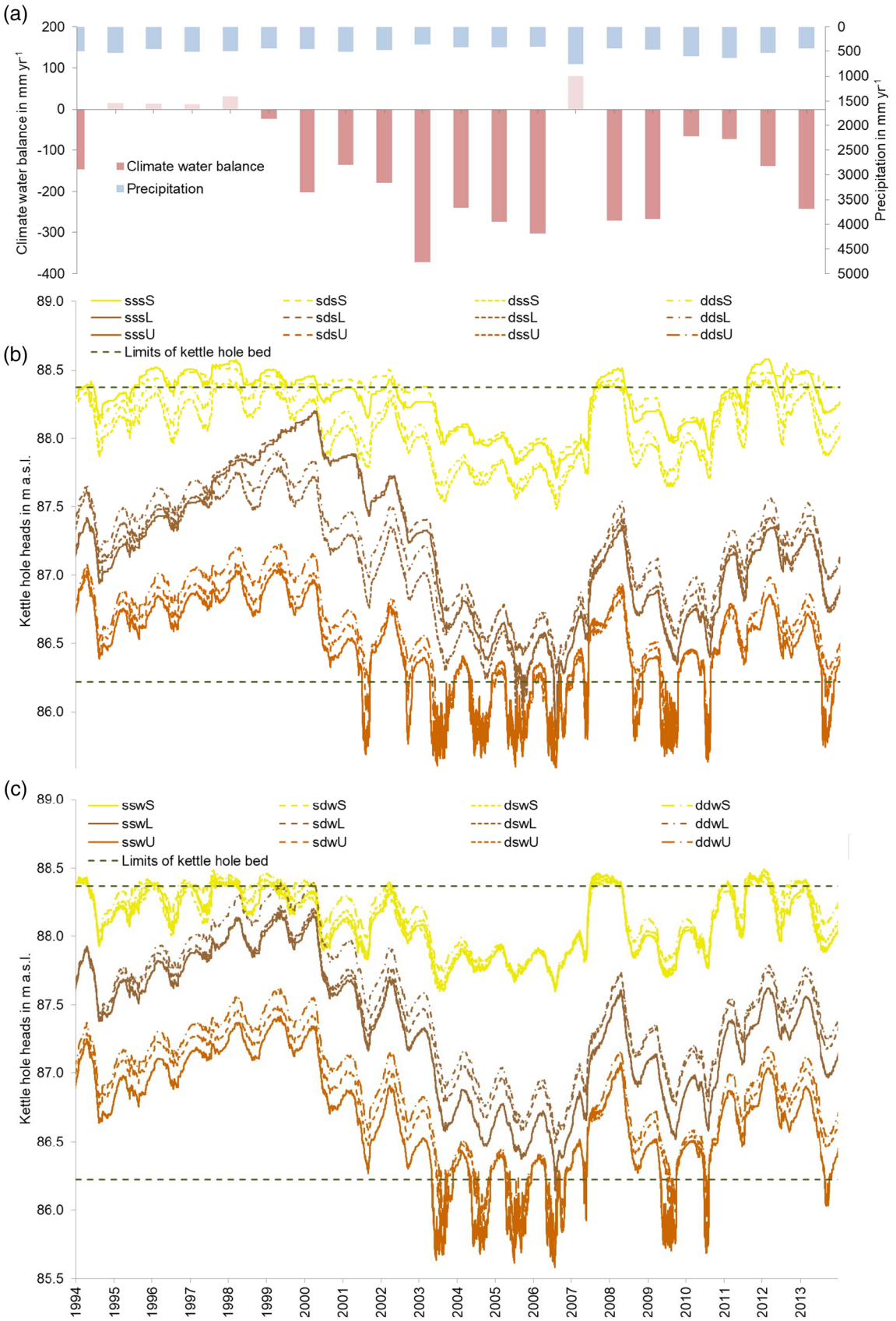

FIGURE 3 Heights of precipitation and of climatic water balance for hydrological years (a) and hydrographs of the kettle hole water level for the model variants with slightly permeable glacial till (b) and weakly permeable glacial till (c).

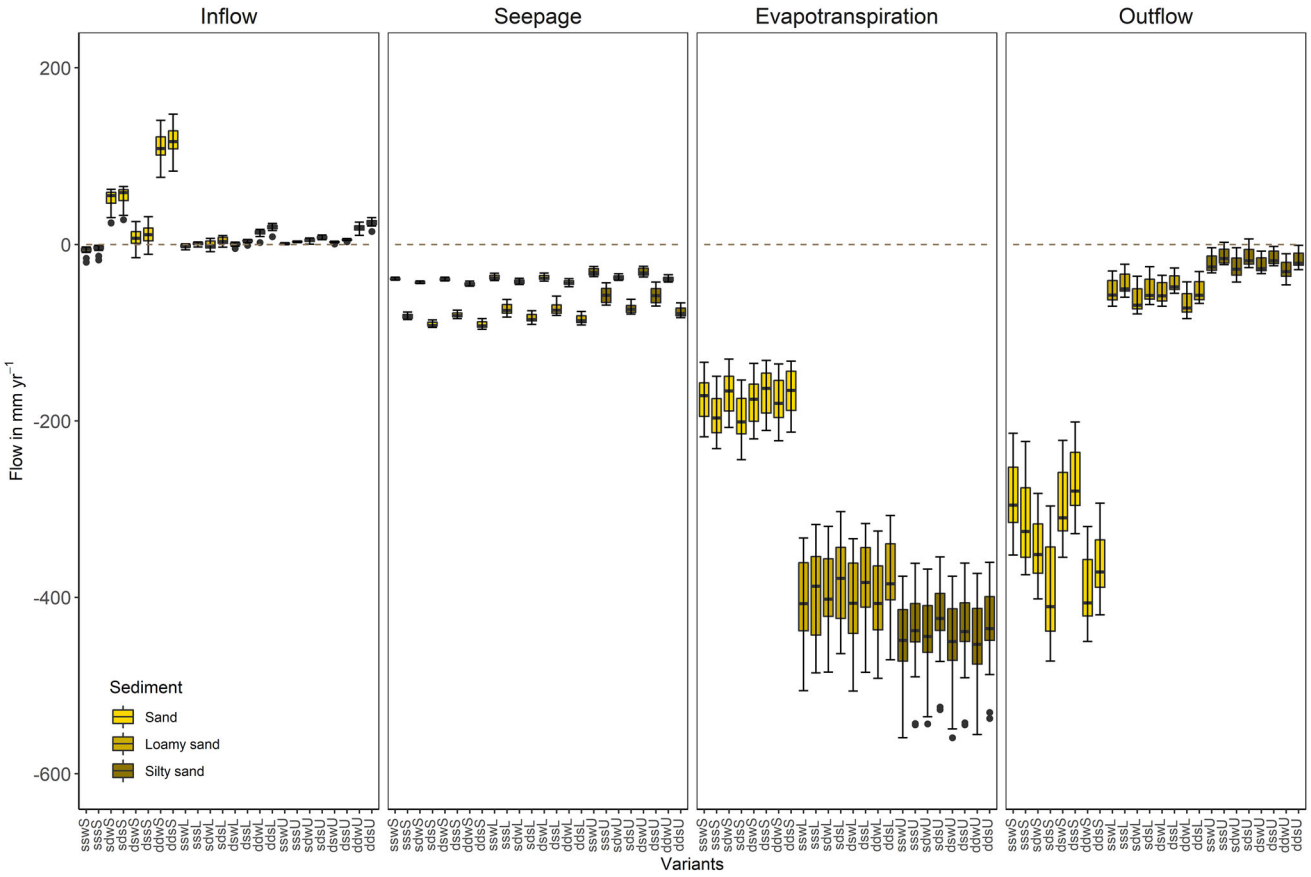

FIGURE 4 Annual water flow rates through the outer boundaries of the model domain for all 24 model variants (boxes indicate the quartiles; the whiskers indicate minimum and maximum values).

also had less effect on lateral runoff, which averaged 332 mm y^{-1} (Figure 4). At the same time, however, the lowest water level fluctuations were achieved in the kettle hole (Figure 5).

The maximum water level fluctuations over the entire period ranged from 0.78 m to 0.94 m for the variant with pure sand, from 1.57 m to 2.38 m for the variant with loamy sand, and from 1.38 m to 1.85 m for the variant with silty sand. In the same order, the maximum intra-annual water level variations ranged from 0.05–0.66 m, 0.13–0.81 m, and 0.13–1.12 m, respectively (Table 4).

As the water storage capacity increases and the permeability of the aquifer decreases, the variability of the water level and the degree of its dynamics increase. This is reflected in the intra-annual water level variations (Table 4).

3.2 | Effects of hydraulic conductivity and thickness of glacial till layer on the water exchange components

In the case of the slightly permeable glacial till, a maximum seepage of about 100 mm y^{-1} was observed, while for the weakly permeable glacial till only up to 50 mm y^{-1} left the model area (Figure 4). As a result, slightly higher water levels were found in both the kettle hole and aquifer for 10 of the 12 comparisons (Figure 5). The exceptions were variants with a static lateral boundary condition and pure sand. Even though all losses through the model boundaries are higher compared to the variants with the weakly permeable glacial till, the variants with the slightly permeable glacial till resulted in higher water levels in the kettle hole and in the adjacent shallow aquifer. In the case of the shallow weakly permeable glacial drift, the duration with reversed groundwater flow was twice as high (337 vs. 157 days) as in the same simulation with the slightly permeable glacial drift. The increase in water availability combined with the high-potential evapotranspiration at kettle hole resulted in slightly lower water levels in the kettle hole.

The thicker the glacial till, the lower the deep seepage rate. Depending on the model variant, the average seepage varied between 5 and 20 mm y^{-1}. A similar behaviour occurred at the outlet of the model domain, where the average seepage varied between 1 and 100 mm y^{-1}. The same effect can be observed in the resulting water levels. In contrast to the shallower glacial till, the water level of the kettle hole rose by up to 0.2 m on average in simulations with a deeper glacial till.

In these cases, simulated water levels were strongly influenced by the location and course of the interface between the aquifer and aquitard (Figure 2).

With respect to water level variation, the deviations between the variants with slightly and weakly permeable glacial till decreased as the grain size of the top sediment layer was reduced (Table 4).

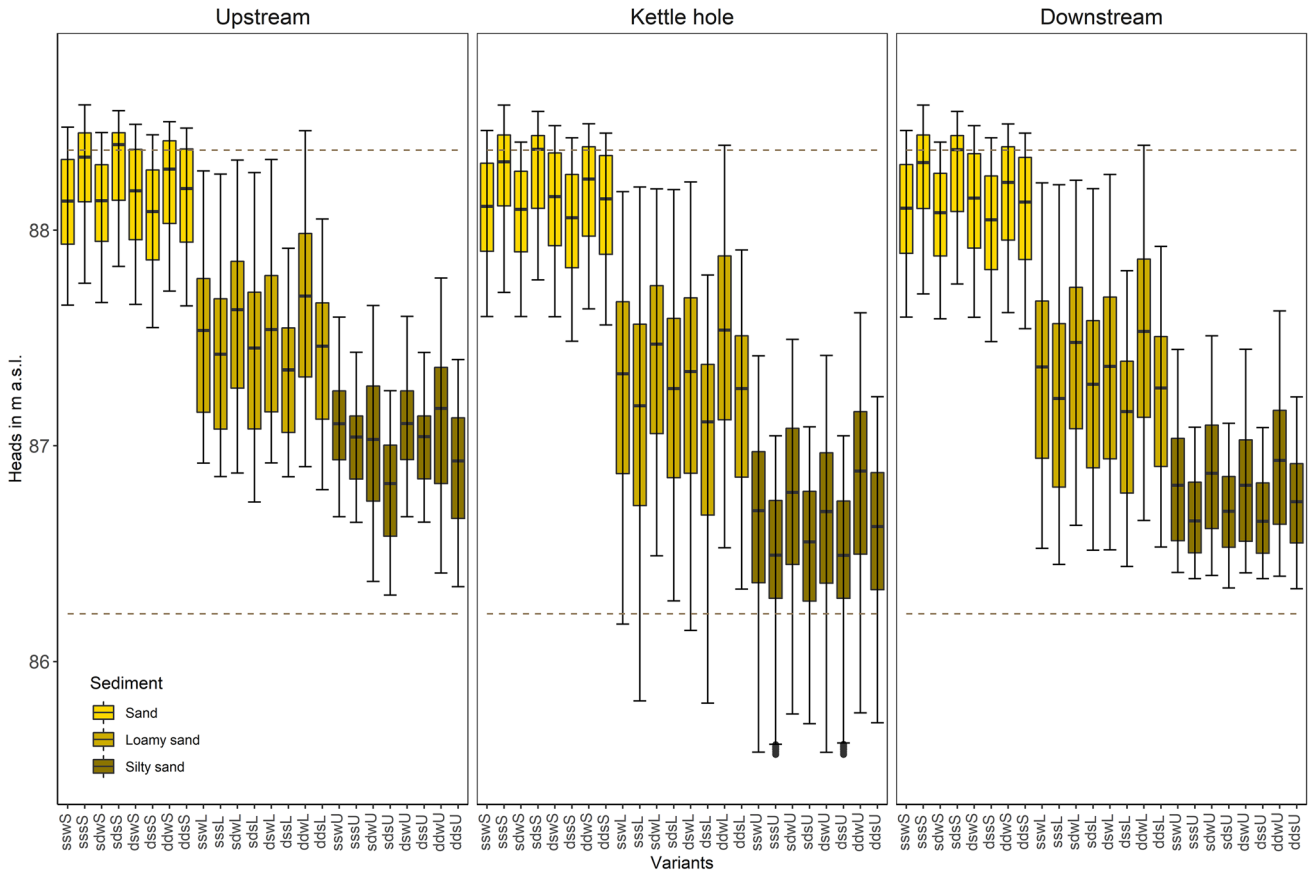

FIGURE 5 Water level fluctuation within the kettle hole (middle) and in the up- and down-gradient fringe (left, right) for all model variants (box plots) in comparison to the bathymetry of the kettle hole (dashed lines).

TABLE 4 Range of maximum intra-annual water level fluctuation and maximum water level change over the simulation period (1994–2013) for different sediment texture classes

Maximum water level fluctuation (m)								
Pure sand			**Loamy sand**			**Silty sand**		
Variant	Intra-annual	Overall	Variant	Intra annual	Overall	Variant	Intra annual	Overall
sssS	0.14–0.60	0.87	sssL	0.18–0.76	2.38	sssU	0.14–1.11	1.48
sdsS	0.05–0.48	0.78	sdsL	0.15–0.71	1.91	sdsU	0.13–0.82	1.38
dssS	0.18–0.66	0.94	dssL	0.13–0.76	1.98	dssU	0.14–1.12	1.48
ddsS	0.15–0.65	0.89	ddsL	0.14–0.72	1.57	ddsU	0.13–0.86	1.51
sswS	0.16–0.61	0.86	sswL	0.17–0.81	2.01	sswU	0.14–1.09	1.84
sdwS	0.16–0.54	0.81	sdwL	0.16–0.74	1.70	sdwU	0.13–0.84	1.74
dswS	0.16–0.59	0.89	dswL	0.18–0.80	2.08	dswU	0.14–1.09	1.84
ddwS	0.15–0.60	0.86	ddwL	0.20–0.72	1.87	ddwU	0.13–0.88	1.85

3.3 | Effects of the lateral boundary conditions on the water exchange components

The lateral boundaries played a pivotal role in the in- and outflow of the model domain. The greatest influence was exerted by the variants with pure sand (Figure 4), while decreasing permeability resulted in lower flow through the lateral boundaries of the model area. However, the inflow was still somewhat greater for the variants with silty sand as compared to the variants with loamy sand. This can be explained by the significantly increased evapotranspiration of 48 mm y^{-1} on average. This is primarily compensated for by the reduction in water levels, but still has some effect on inflow.

The change in the lateral boundary condition affected intra-annual water level fluctuations by only 0.13 m. The variable head boundary condition almost led to slightly higher average values, except for the "..sU" and "..wS" variants.

3.4 | Water exchange between the kettle hole and the shallow groundwater

Differently parameterized model configurations, resulted in divergent dynamics with a wide range of effects on flow properties. The hydraulic diffusivity, as a quotient of the transmissivity and storage coefficient of the aquifer, always indicates a significantly higher velocity of groundwater movement for pure sand than for the other substrates (Figure 6). With a deeper marl, that is, a thicker aquifer, this velocity increased clearly for all substrates. Depending of the lateral boundary condition, the influence of the permeability of the marl was clearly lower and reversed. Thus, the diffusivity values for the static boundary conditions and weakly permeable marl were mostly below those with slightly permeable marl. The opposite was true for dynamic boundary conditions. However, the sole influence of the lateral boundary conditions, whether static or dynamic, was clearly lowest for all substrates. As expected, all these differences decreased with increasing distance from the kettle hole.

The simulation results indicated that the flow direction and velocity from/to the kettle hole were not stable over time (Table 5). Depending on meteorological conditions, as well as on the site and sediment hydraulic conditions, the groundwater flow direction often reversed in the downstream section.

The frequency with which the flow reversed from the downstream aquifer back to the kettle hole increased with a reduction in the permeability of the top sediment layer. In the variant group with the silty sand, the reversal in the groundwater flow from the downstream aquifer towards the kettle hole ensued on more than 74% of the days of the simulation period. In contrast, this held true only on at most 5% of the days for the variant group with the pure sand (Table 5). Conversely, the flow towards the downstream aquifer happened on at least 95% of days with pure sand, but never arose in two of the model variants with the silty sand. The variant group with loamy sand exhibited intermediate incidences falling between the two extremes resulted from the pure sand and silty sand model variants.

The duration of flow towards the downstream aquifer remained below 300 consecutive days for the loamy and silty sand variant groups, whereas the reversal groundwater flow from the downstream aquifer into the kettle hole appeared over a period of at least a year. The maximum duration of the reversal groundwater flow occurred in response to simulations with the silty sand as the top sediment layer. The results revealed that several years of reversal groundwater flow, sometimes even spanning the entire simulation period, that is, 6940 days. Under these circumstances, a faster rise to groundwater level played an important role, rather than the kettle hole's water level. A noticeable increase in the number of days with reversal

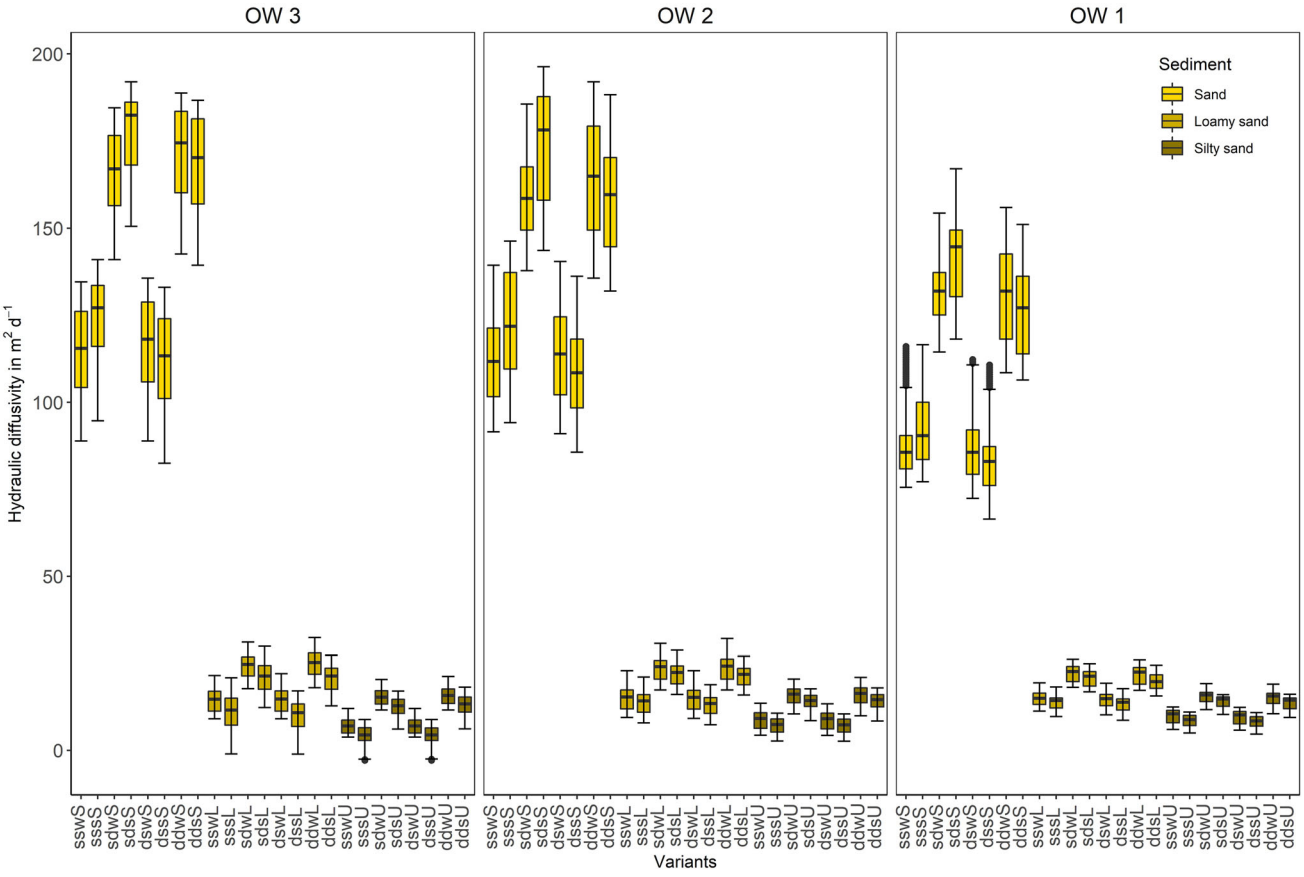

FIGURE 6 Hydraulic diffusivity at the downstream observation wells OW 3, OW 2 and OW 1 for all 24 model variants. Observation wells are positioned at distances of 25 m (OW 3), 80 m (OW 2) and 140 m (OW 1) downstream from the observation well in the kettle hole.

TABLE 5 Frequency of flow directions sorted by the variant groups with pure sand ("… S"), loamy sand ("… L") and silty sand ("… U"). Flow direction from groundwater of the downgradient aquifer to the kettle hole (GW ⇨ KH) and vice versa (KH ⇨ GW)

	Relative frequency of occurrence of water flow in %		Maximum number of consecutive days	
Variant group	**GW ⇨ KH**	**KH ⇨ GW**	**GW ⇨ KH**	**KH ⇨ GW**
"…S"	1 … 5	95 … 99	3 … 35	342 … 1750
"…L"	42 … 85	15 … 58	396 … 2175	96 … 267
"…U"	74 … 100	0 … 26	2014 … 6940	0 … 232

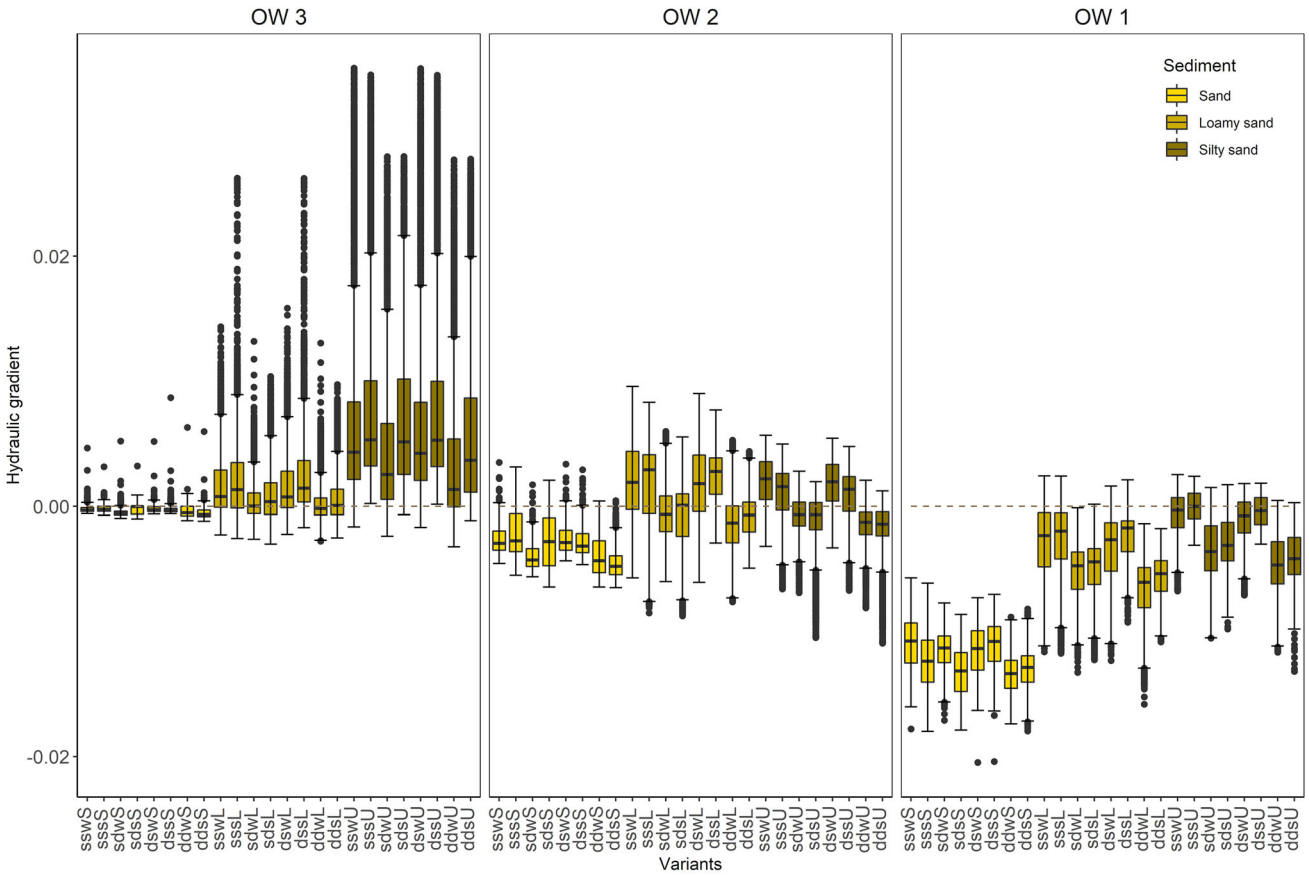

FIGURE 7 Hydraulic gradients between observation wells OW(KH) and OW 3 (OW 3), OW 3 and OW 2 (OW 2) and OW 2 and OW1 (OW 1) for all 24 model variants. Positive values indicate groundwater flow from the downstream aquifer towards the kettle hole. Observation wells are positioned at distances of 25 m (OW 3), 80 m (OW 2) and 140 m (OW 1) downstream from the observation well in the kettle hole.

groundwater flow was detected owing to low-hydraulic conductivity. In contrast, the variant group with the pure sand showed a clear flow-through characteristic, which could potentially influence the groundwater domain even at larger distances. Nonetheless, the flow-through behaviour ceased due to temporary flow reversals (lasting from 3 to 35 days) that appeared during and after precipitation events.

What can be confirmed, in an environment with a slightly sloping topography, is that there were behavioural patterns that were subject to seasonal fluctuations and related to the water table. The hydraulic gradients in the observation wells located at different distances in the down-gradient direction demonstrate this (Figure 7). When the water levels were high, the kettle hole represented a flow-through system, albeit with the reversal flows that occurred only during short storm events. A direct relationship could be discerned between the duration of the groundwater flow reversal and the duration of the storm event. This was supported further by a reduction in the hydraulic conductivity of the top sediment layer. The groundwater flow reversal often extended to at least 80 metres in the down-gradient direction. A considerable increase in reversal flows was also seen in variants with a shallow interface between the top sediment layer and the glacial till. The only exceptions were sediments with high-hydraulic conductivity. The aforementioned flow-through behaviour of the variant group with the pure sand became more obvious, leading to a highly apparent water exchange in the immediate vicinity of the kettle hole up to a distance of 25 m. In periods when the kettle hole's water level declined accompanied by the low-hydraulic conductivity of the top

sediment layer, the groundwater flow reversals prevailed, as demonstrated by the very steep gradients in Figure 7. Depending on the sediment hydraulic properties and boundary conditions, this influence extended to a maximum of 140 metres. Moreover, the influence was greater when there was a shallow interface between the sediment and the glacial till. Similarly, steeper gradients occurred when the top sediment was thin. A medium kettle hole water level provoked the groundwater flow towards the kettle hole and vice versa, depending on the hydraulic head conditions during the preceding period.

3.5 | Mass transfer and exchange

The spatial distribution and the share of the water originating from the kettle hole in the groundwater domain were analysed at two different time steps under the selected model variants "ddsS", "ddsL" and "dssU" (Figure 8). Examining the flow direction, the variants "ddsS" and "dssU" represented the two extremes of all variants, whereas "ddsL" exhibited medium flow conditions. It became obvious that in the case of the variant with the pure sand, the solute spread across the entire model domain to a downstream distance of more than 100 m. However, for variants with loamy and silty sand, the water exchange zone was restricted to the vicinity of the kettle hole, that is, 50 m. Compared to the variants with loamy and silty sand, the long period with flow-through conditions in conjunction with a high-hydraulic conductivity led to a high dilution effect. On the other hand, the prolonged period of revers groundwater flow even in the case of the loamy sand (Table 5) and the high-evapotranspiration rates (Figure 4) caused a concentrated solute transport towards the surface and down to a greater depth. In periods with a large deficit in precipitation, relative to the potential evapotranspiration, such as in 2003 (Figure 3), the spatial distribution of the solute concentrated on the top sediment layer and along the interface of the glacial till. In combination with a low-groundwater level and a low-water level within the kettle hole, deep seepage through the glacial till was not observed. In periods with higher precipitation rates, such as in 2012, the solute concentration was diluted due to the percolating water (Figure 8, top right). In the case of "ddsS", the solute also flowed along the surface

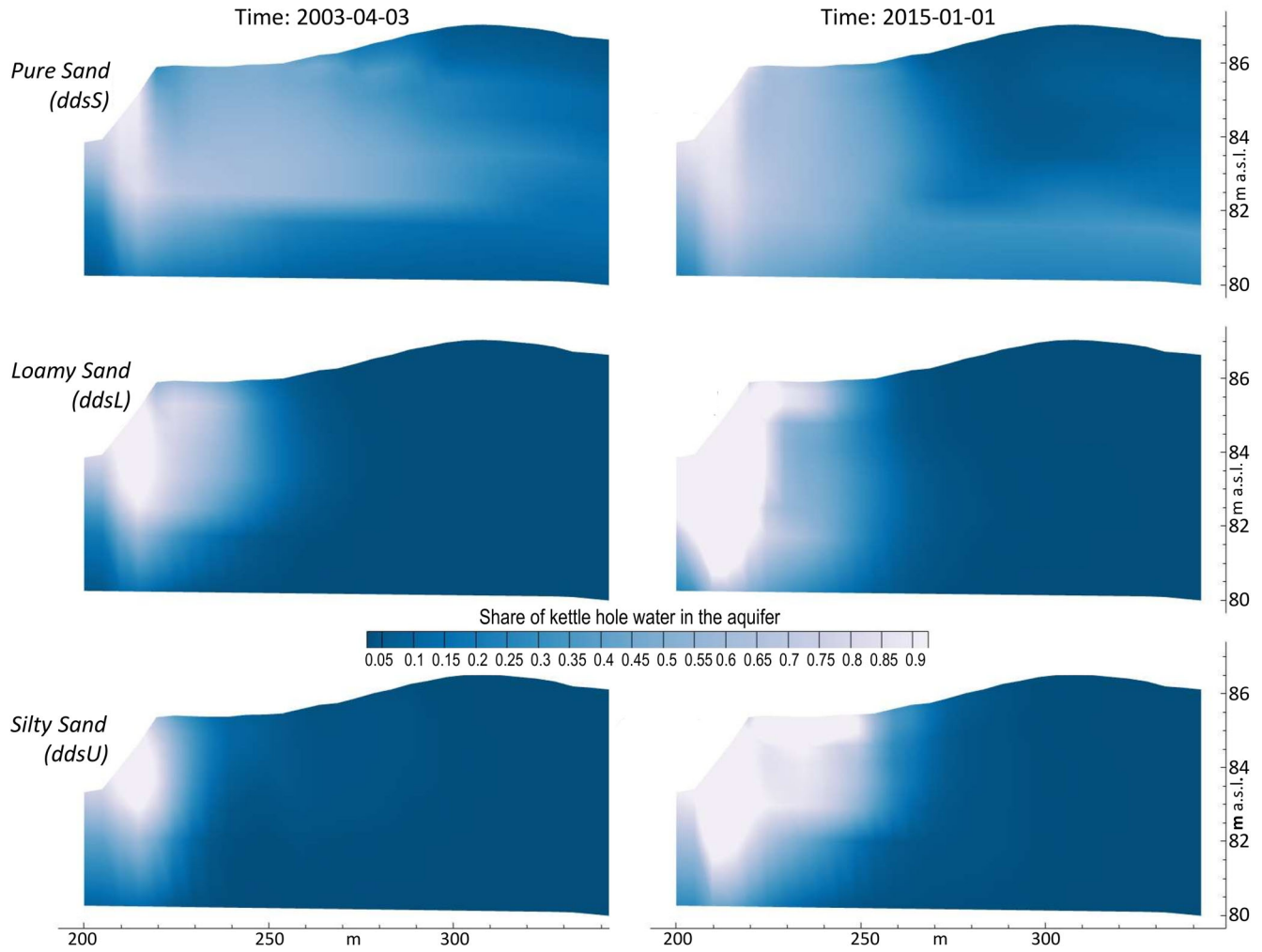

FIGURE 8 Spatial distribution of the kettle hole water in the down-gradient aquifer at two different points in time and for the three selected model variants ddsS, ddsL and ddsU.

of the glacial till, albeit at a substantially lower concentration. Relative to 2003, the higher water levels in 2015 led to greater seepage rates, allowing the solute to also infiltrate into the glacial till. Moreover, in the model variants with loamy and silty sand, the seasonal variability in the flow direction caused the solute to disperse over a larger area (Figure 8, bottom right).

4 | DISCUSSION

4.1 | Model design

This numerical experiment aimed at exploring the spatio-temporal flux exchange between a kettle hole in the northeast of Brandenburg, Germany and its adjacent shallow groundwater system under a range of plausible model variants capturing various porous media hydraulic properties and boundary conditions.

In order to limit the set of possible spatial combinations and to cope with this complexity described for example, by Gerke et al. (2010) or Kleeberg, Neyen, Schkade, et al. (2016), the decision was made to use three suitable, sufficiently permeable sediment types, simplified as a homogeneous, isotropic upper sediment layer over an equally homogeneous, isotropic marl. At a very similar site, Ehrhardt et al. (2022) recently demonstrated anisotropic conditions in a haplic Regosol (calcareous) soil profile. Most of their anisotropy rates were in the lower range of the assumptions made by Nield et al. (1994). It can thus be assumed that the horizontal flow component from the kettle hole towards the groundwater and revers was underestimated somewhat. However, the seepage boundary condition assumed to take place at the lower model boundary can also influence these groundwater flow movements on the marl sediments, which form the bottom of the layer of the modelling domain. This became more evident, for example, through the influence of marl permeability on hydraulic diffusivity (as illustrated Figure 6). In view of the high variability of hydrogeomorphic site conditions, further considerations were included (see Section 2.4) to capture a wide range of possible subsurface conditions without modelling specific features.

However, in comparison to a 3D approach, our quasi-2D model approach bearing less complexity made it possible to constrain further uncertainties with respect to the boundary conditions. Nonetheless, the results of the applied quasi 2D model can still be compared with those of a 3D model approach, at least for shallow small water bodies like kettle holes with a circular geometry with which groundwater in exchange is (Townley & Trefry, 2000). It should be note that the 2D modelling approach becomes less and less useful as the geometry of the water body becomes longer and thinner along the groundwater flow direction, as reported by Nield et al. (1994). Under all of the model variants, owing to both a lower sediment permeability and consistently high static pressure heads at the model boundaries, the groundwater lateral flow from the kettle hole towards the aquifer was impeded. It holds especially true for model variants with pure sand rather than the model variants with loamy or silty sand. Overall, however, the simulated water level fluctuations in the kettle hole were found to be consistent with the findings of Heagle et al. (2013) and Lehsten et al. (2011). The latter found a maximum intra-annual water level fluctuation of about one meter. This was exceeded, by up to 11%, only by the four silty sand model variants with the static boundary conditions and shallow aquitard. Similarly, the observed water level fluctuation of no more than two metres over a period of several years was exceeded only by three loamy sand variants with static boundary conditions, albeit in one case by up to 19%.

At such high-water levels, fill-spill mechanism (Hayashi et al., 2016, Shaw et al., 2012) can occur, which means the water overtops the kettle hole (i.e., spills) and is then flowed towards downstream (Shaw et al., 2013). A process of this kind was probably recorded in Figure 1. It can be mainly resulted from heavy storm events that occur in winter on frozen soils or in summer on saturated soils.

4.2 | Groundwater flow reversal

The simulation results emphasized that precipitation and evapotranspiration not only determine the water balance of the kettle hole but also have a major impact on the degree of mass exchange from the kettle hole in the direction of the downstream aquifer. This can be seen in atmospheric fluxes, which is in accordance with the findings of Ferone and Devito (2004). The topology of the landscape elements and meteorological conditions strongly control the hydraulic gradient, which in turn affects the intensity of water exchange between the kettle hole and the shallow groundwater domain.

Potential evapotranspiration from the vegetation in and around a kettle hole is much higher than that of the adjacent crop field area (e.g., Pauliukonis & Schneider, 2001). In consequence, it causes an impact on kettle hole water levels on the one hand and the hydraulic gradient between a kettle hole and its adjoining groundwater (Figure 7) on the other hand. As a result, the groundwater flow from the direction of the kettle hole stagnates and may also reverse. There are many studies that have investigated the stagnation and reversal of groundwater flow; for instance, studies focusing on the groundwater flow reversal in bogs or peatlands (e.g., Devito, 1997, Ferone & Devito, 2004, Fraser et al., 2001), investigations placing an emphasis on wetlands (e.g., Pyzoha et al., 2008; Sun et al., 2006) and studies concentrating on lakes (e.g., Cheng & Anderson, 1994; Sacks et al., 1992).

Consistent with observations by Ferone and Devito (2004) at a lowland pond, however, strong storm events also resulted in short-term groundwater flow reversals. Because of the low porosity of the aquifer sediment, the groundwater head rises more rapidly relative to the kettle hole water level. Simultaneous or subsequent higher evaporation losses within the kettle hole can increase the hydraulic gradient. In the present study, such groundwater reversal flows occurred only in the initial phase of rewetting.

We were able to show that the hydraulic properties of the aquifer sediments have a significant influence on the groundwater flow reversal, driven by the effects described above. Our findings demonstrated

that groundwater flow reversals occurred more frequently as the aquifer permeability decreases compared with the relatively high-permeability of pure sand (see Table 5). Thus, in the variant group with the silty sand, the reverse groundwater flow from the downstream aquifer into the kettle hole continued over the entire simulation period. Similarly, the model variants with the loamy sand underwent periodic fluctuations. Our findings are not consistent with investigations by Sacks et al. (1992) and Ferone and Devito (2004), who demonstrated that only a rise in the groundwater water level during the wet seasons or periods induced a local reversal in the groundwater flow. Nonetheless, in some studies (e.g., Fraser et al., 2001), groundwater flow reversal was necessarily associated with drought conditions. Although in the current study a dominant flow-through system was only observed for the variant group with pure sand, a kettle holes show often a dominant flow-through system (e.g., Vyse et al., 2020).

Our results demonstrated that depending on the hydraulic properties of the subsurface sediments, the interaction between a kettle hole (pond or small lake) and its adjoining shallow groundwater is highly variable in time and space, instead of the rather static system that is commonly expected. However, the range of these effects presented in this study is likely to be somewhat smaller given the naturally occurring heterogeneities in aquifer properties.

The position of a kettle hole in the regional groundwater flow system should also be taken into account in order to be able to evaluate possible groundwater flow reversals and their effects. This is a result of several studies on lakes (Cheng & Anderson, 1994; Ferone & Devito, 2004; Heagle et al., 2007; Sacks et al., 1992; Smith & Townley, 2002).

Irrespective of this, our study and any other modelling approaches are necessarily based on simplified assumptions and thus do not grasp the full range of heterogeneities that are found, in particular, in postglacial landscapes. However, our results clearly call for particular attention to be paid to these reverse groundwater flows when studying water quality in kettle holes as well as their interactions with their adjacent groundwater system. Reverse groundwater flows can influence the kettle hole's matter balance and function as a habitat. Substances recently transported from the kettle hole into the groundwater domain can return, and materials leached from the soil that would otherwise enter downstream waters can be transported into the kettle hole. This affects a large number of kettle holes or potholes, which have a relatively similar geological and geomorphological genesis in glacially influenced areas of the Earth. It should be noted that findings of this study can be useful for the Prairie Pothole Region in North America, where thousands of shallow potholes show geologically and geomorphologically relatively similar genesis to kettle holes in North Central Europe. Thus, modelling flow and solute transport between kettle holes or potholes and their adjoining shallow groundwater systems using mechanistic hydrological models requires intensive soil and geological explorations, depending on the size and complexity of the modelling area. This holds true especially for postglacial landscapes, where undulating topography and variegated soil and aquifer sediments create a highly heterogeneous continuum. For this reason, in the light of the findings of the present study, we specify different model variants, comprising a wide yet well-founded range of porous material properties. As a result, a wide variety of model outputs, represented as model uncertainty, are presented and can be analysed for kettle holes when modelling flow/solute using a demanding but stat-of-the-art hydrological model such as HGS.

5 | CONCLUSIONS

The kettle holes distributed across Pleistocene landscapes are hydrologically intricate systems. The hydrological relationships between them and the adjoining shallow groundwater system are still poorly documented. Due to the extreme heterogeneity of Pleistocene landscapes, especially with respect to soil hydraulic properties, considerable uncertainties are expected when modelling such systems. Therefore, a modelling scheme was proposed in the present study that is based on a wide range of model variants comprising a reasonable uncertainty range. The predefined variants were integrated into HGS, allowing us to investigate the transient flux exchange between a kettle hole in the northeast of Brandenburg, Germany and its adjacent shallow groundwater system.

Our results clearly indicated that kettle holes and shallow groundwater can be much more closely and dynamically linked than previously thought. The groundwater flow direction in the downstream part of the groundwater system can exhibit reversals for periods of up to several years and can extend a distance of more than 140 m downstream of the kettle hole. Our findings demonstrate that the reversal in the groundwater flow occurs particularly in regions where the uppermost aquifer has low-hydraulic conductivity. The very high evapotranspiration of the aquatic vegetation encircling kettle holes, alongside heavy storm events, can repeatedly reverse the flow from the groundwater domain towards kettle holes, causing solute turnover within the kettle hole. This is particularly prevalent in dry periods with medium to low-water levels within the kettle hole and a negative climate water balance. Based on the results obtained from 24 model configurations/variants, this study has demonstrated that shallow groundwater flow reversals are not exclusively a consequence of seasonal effects.

A necessary simplification considered in this modelling approach was made with the aim of simulating reality using a two-dimensional model. The reduction in permeability caused by siltation was also not taken into consideration, although most kettle holes contain bottom sediments formed by internal accumulation. The influence of those sediments on surface water–groundwater interactions can be substantial, especially in the case of low permeability. However, this also depends on the spatial distribution of the clogging over the bottom sediments of kettle holes. Furthermore, we assumed that preferential flow paths, such as macropore flow paths, are negligible for soil water movement due to the sandy texture of the modelling site. The consequences of these prior assumptions could not be fully examined in this numerical experiment. Thus, the findings can be generalized only to a very limited degree. Nonethelessthey certainly helps to set the problem in a suitable framework.

Kettle holes should be considered as zones at high risk of groundwater contamination if they are located near croplands. As a result, leaching and transporting of fertilizers from croplands towards kettle holes and their subsequent redistribution to the river network may lower the water quality of downstream waters. Periods of groundwater flow reversal in the adjacent downstream aquifer may intensify the risk of contamination, which certainly needs to be taken into account. Thus, even from the groundwater protection aspect alone, the ecological and hydrological functions of countless kettle holes in the Late Pleistocene landscapes are of great importance.

ACKNOWLEDGEMENTS

We thank our colleagues working on the Leibniz Association's LandScape project for supporting this work with their data and constructive feedback. The data used are listed in the references and tables.

DATA AVAILABILITY STATEMENT

The data that support the findings of this study are openly available in Open Research Data at https://open-research-data.zalf.de/default.aspx, reference number 10.4228/ZALF.1992.233.

ORCID

Jörg Steidl https://orcid.org/0000-0002-6599-0450

REFERENCES

Akbari, F., Shourian, M., & Moridi, A. (2022). Assessment of the climate change impacts on the watershed-scale optimal crop pattern using a surface-groundwater interaction hydro-agronomic model. *Agricultural Water Management*, *265*, 107508.

Allen, R. G., Pereira, L. S., Raes, D., & Smith, M. (1998). FAO irrigation and drainage paper No. 56. Rome: Food and agriculture Organization of the United Nations, 56, e156.

Amado, A. A., Politano, M., Schilling, K., & Weber, L. (2018). Investigating hydrologic connectivity of a drained prairie pothole region wetland complex using a fully integrated, physically-based model. *Wetlands*, *38*, 233–245.

Anderson, M. P., & Munter, J. A. (1981). Seasonal reversals of groundwater flow around lakes and the relevance to stagnation points and lake budgets. *Water Resources Research*, *17*, 1139–1150.

Aquanty. (2013). *HGS 2013 - hydro geo sphere user manual*. Waterloo.

Bailey, R. T., Wible, T. C., Arabi, M., Records, R. M., & Ditty, J. (2016). Assessing regional-scale spatio-temporal patterns of groundwater–surface water interactions using a coupled SWAT-MODFLOW model. *Hydrological Processes*, *30*, 4420–4433.

Berthold, S., Bentley, L. R., & Hayashi, M. (2004). Integrated hydrogeological and geophysical study of depression-focused groundwater recharge in the Canadian prairies. *Water Resources Research*, *40*, 14.

Cheng, X., & Anderson, M. P. (1994). Simulating the influence of lake position on groundwater fluxes. *Water Resources Research*, *30*, 2041–2049.

Cohen, M. J., Creed, I. F., Alexander, L., Basu, N. B., Calhoun, A. J. K., Craft, C., D'amico, E., Dekeyser, E., Fowler, L., Golden, H. E., Jawitz, J. W., Kalla, P., Kirkman, L. K., Lane, C. R., Lang, M., Leibowitz, S. G., Lewis, D. B., Marton, J., Mclaughlin, D. L., … Walls, S. C. (2016). Do geographically isolated wetlands influence landscape functions? *Proceedings of the National Academy of Sciences of the United States of America*, *113*, 1978–1986.

Crundwell, M. E. (1986). A review of hydrophyte evapotranspiration. *Revue d'hydrobiologie tropicale*, *19*(3–4), 215–232.

der Kamp, V., & Hayashi, M. (2009). Groundwater-wetland ecosystem interaction in the semiarid glaciated plains of North America. *Hydrogeology Journal*, *17*, 203–214.

Derby, N. E., & Knighton, R. E. (2001). Field-scale preferential transport of water and chloride tracer by depression-focused recharge. *Journal of Environmental Quality*, *30*, 194–199.

Devito, K. J., Waddington, J. M., & Branfireun, B. A. (1997). Flow reversals in peatlands influenced by local groundwater systems. *Hydrological Processes*, *11*, 103–110.

Downing, J. A. (2010). Emerging global role of small lakes and ponds: Little things mean a lot. *Limnetica*, *29*, 9–24.

Ehrhardt, A., Berger, K., Filipović, V., Wöhling, T., Vogel, H.-J., & Gerke, H. H. (2022). Tracing lateral subsurface flow in layered soils by undisturbed monolith sampling, targeted laboratory experiments, and model-based analysis. *Vadose Zone Journal*, *21*, e20206.

Ferone, J. M., & Devito, K. J. (2004). Shallow groundwater–surface water interactions in pond–peatland complexes along a Boreal Plains topographic gradient. *Journal of Hydrology*, *292*, 75–95.

Fraser, C. J. D., Roulet, N. T., & Lafleur, M. (2001). Groundwater flow patterns in a large peatland. *Journal of Hydrology*, *246*, 142–154.

Gerke, H. H., Koszinski, S., Kalettka, T., & Sommer, M. (2010). Structures and hydrologic function of soil landscapes with kettle holes using an integrated hydropedological approach. *Journal of Hydrology*, *393*, 123–132.

Golden, H. E., Lane, C. R., Amatya, D. M., Bandilla, K. W., Kiperwas, H. R., Knightes, C. D., & Ssegane, H. (2014). Hydrologic connectivity between geographically isolated wetlands and surface water systems: A review of select modeling methods. *Environmental Modelling & Software*, *53*, 190–206.

Groh, J., Diamantopoulos, E., Duan, X., Ewert, F., Herbst, M., Holbak, M., Kamali, B., Kersebaum, K.-C., Kuhnert, M., Lischeid, G., Nendel, C., Priesack, E., Steidl, J., Sommer, M., Pütz, T., Vereecken, H., Wallor, E., Weber, T. K. D., Wegehenkel, M., … Gerke, H. H. (2020). Crop growth and soil water fluxes at erosion-affected arable sites: Using weighing lysimeter data for model intercomparison. *Vadose Zone Journal*, *19*, e20058.

Hayashi, M., van der Kamp, G., & Rosenberry, D. O. (2016). Hydrology of prairie wetlands: Understanding the integrated surface-water and groundwater processes. *Wetlands*, *36*, S237–S254.

Hayashi, M., van der Kamp, G., & Rudolph, D. L. (1998). Water and solute transfer between a prairie wetland and adjacent uplands, 2. Chloride cycle. *Journal of Hydrology*, *207*, 56–67.

Hayashi, M., van der Kamp, G., & Schmidt, R. (2003). Focused infiltration of snowmelt water in partially frozen soil under small depressions. *Journal of Hydrology*, *270*, 214–229.

Heagle, D., Hayashi, M., & Kamp, G. V. D. (2013). Surface–subsurface salinity distribution and exchange in a closed-basin prairie wetland. *Journal of Hydrology*, *478*, 1–14.

Heagle, D. J., Hayashi, M., & Van Der Kamp, G. (2007). Use of solute mass balance to quantify geochemical processes in a prairie recharge wetland. *Wetlands*, *27*, 806–818.

Kalettka, T., & Rudat, C. (2006). Hydrogeomorphic types of glacially created kettle holes in north-East Germany. *Limnologica - Ecology and Management of Inland Waters*, *36*, 54–64.

Kalettka, T., Rudat, C., & Quast, J. (2001). Potholes in northeast German agro-landscapes: Functions, land use impacts, and protection strategies. *Ecological Studies*, *147*, 291–298.

Kazmierczak, E. (1997). The vegetation of kettle-holes in Central Poland. Sv. växtgeografiska sällsk.

Kim, K. B., Kwon, H.-H.. & Han, D. (2018). Exploration of warm-up period in conceptual hydrological modelling. *Journal of Hydrology*, *556*, 194–210.

Kleeberg, A., Neyen, M., & Kalettka, T. (2016). Element-specific downward fluxes impact the metabolism and vegetation of kettle holes. *Hydrobiologia*, *766*, 261–274.

Kleeberg, A., Neyen, M., Schkade, U.-K., Kalettka, T., & Lischeid, G. (2016). Sediment cores from kettle holes in NE Germany reveal recent impacts of agriculture. *Environmental Science and Pollution Research*, *23*, 7409–7424.

Kristensen, K., & Jensen, S. (1975). A model for estimating actual evapotranspiration from potential evapotranspiration. *Hydrology Research*, *6*, 170–188.

Lehsten, D., von Asmuth, J. R., & Kleyer, M. (2011). Simulation of water level fluctuations in kettle holes using a time series model. *Wetlands*, *31*, 511–520.

Leibowitz, S. G. (2015). Geographically isolated wetlands: Why we should keep the term. *Wetlands*, *35*, 997–1003.

Lischeid, G., & Kalettka, T. (2012). Grasping the heterogeneity of kettle hole water quality in Northeast Germany. *Hydrobiologia*, *689*, 63–77.

Lischeid, G., Kalettka, T., Holländer, M., Steidl, J., Merz, C., Dannowski, R., Hohenbrink, T., Lehr, C., Onandia, G., Reverey, F., & Pätzig, M. (2018). Natural ponds in an agricultural landscape: External drivers, internal processes, and the role of the terrestrial-aquatic interface. *Limnologica*, *68*, 5–16.

Lischeid, G., Kalettka, T., Merz, C., & Steidl, J. (2016). Monitoring the phase space of ecosystems: Concept and examples from the Quillow catchment, Uckermark. *Ecological Indicators*, *65*, 55–65.

Liu, G., Schwartz, F. W., Wright, C. K., & Mcintyre, N. E. (2016). Characterizing the climate-driven collapses and expansions of wetland habitats with a fully integrated surface–subsurface hydrologic model. *Wetlands*, *36*, 287–297.

Logan, W. S., & Rudolph, D. L. (1997). Microdepression-focused recharge in a coastal wetland, La Plata, Argentina. *Journal of Hydrology*, *194*, 221–238.

Lorenz, S., Rasmussen, J. J., Suss, A., Kalettka, T., Golla, B., Horney, P., Stahler, M., Hommel, B., & Schafer, R. B. (2017). Specifics and challenges of assessing exposure and effects of pesticides in small water bodies. *Hydrobiologia*, *793*, 213–224.

Mclaren, R. G. (2008). GRID BUILDER — A pre-processor for 2D, triangular element, finite-element programs. *Groundwater Simulations Group*, *2008*.

Merz, C., & Steidl, J. (2015). Data on geochemical and hydraulic properties of a characteristic confined/unconfined aquifer system of the younger Pleistocene in Northeast Germany. *Earth System Science Data*, *7*, 109–116.

Mitsch, W. J., & Gosselink, J. G. (2015). *Wetlands*. Wiley.

Mushet, D. M., Calhoun, A. J. K., Alexander, L. C., Cohen, M. J., Dekeyser, E. S., Fowler, L., Lane, C. R., Lang, M. W., Rains, M. C., & Walls, S. C. (2015). Geographically isolated wetlands: Rethinking a misnomer. *Wetlands*, *35*, 423–431.

Neff, B. P., & Rosenberry, D. O. (2018). Groundwater connectivity of upland-embedded wetlands in the prairie pothole region. *Wetlands*, *38*, 51–63.

Nield, S. P., Townley, L. R., & Barr, A. D. (1994). A framework for quantitative analysis of surface water-groundwater interaction: Flow geometry in a vertical section. *Water Resources Research*, *30*, 2461–2475.

Nitzsche, K. N., Kalettka, T., Premke, K., Lischeid, G., Gessler, A., & Kayler, Z. E. (2017). Land-use and hydroperiod affect kettle hole sediment carbon and nitrogen biogeochemistry. *Science of the Total Environment*, *574*, 46–56.

Parsons, D. F., Hayashi, M., & Van Der Kamp, G. (2004). Infiltration and solute transport under a seasonal wetland: Bromide tracer experiments in Saskatoon, Canada. *Hydrological Processes*, *18*, 2011–2027.

Pätzig, M., Kalettka, T., Glemnitz, M., & Berger, G. (2012). What governs macrophyte species richness in kettle hole types? A case study from Northeast Germany. *Limnologica*, *42*, 340–354.

Pauliukonis, N., & Schneider, R. (2001). Temporal patterns in evapotranspiration from lysimeters with three common wetland plant species in the eastern United States. *Aquatic Botany*, *71*, 35–46.

Premke, K., Attermeyer, K., Augustin, J., Cabezas, A., Casper, P., Deumlich, D., Gelbrecht, J., Gerke, H. H., Gessler, A., Grossart, H.-P., Hilt, S., Hupfer, M., Kalettka, T., Kayler, Z., Lischeid, G., Sommer, M., & Zak, D. (2016). The importance of landscape diversity for carbon fluxes at the landscape level: Small-scale heterogeneity matters. *WIREs Water*, *3*, 601–617.

Pyzoha, J. E., Callahan, T. J., Sun, G., Trettin, C. C., & Miwa, M. (2008). A conceptual hydrologic model for a forested Carolina bay depressional wetland on the coastal plain of South Carolina, USA. *Hydrological Processes*, *22*, 2689–2698.

Sacks, L. A., Herman, J. S., Konikow, L. F., & Vela, A. L. (1992). Seasonal dynamics of groundwater-lake interactions at Doñana National Park, Spain. *Journal of Hydrology*, *136*, 123–154.

Schaap, M. G., Leij, F. J., & van Genuchten, M. T. (2001). ROSETTA: A computer program for estimating soil hydraulic parameters with hierarchical pedotransfer functions. *Journal of Hydrology*, *251*, 163–176.

Schweizer, V. (2012). Wörterbuch der Geologie/dictionary of geology.

Semiromi, T., & Koch, M. (2019). Analysis of spatio-temporal variability of surface–groundwater interactions in the Gharehsoo river basin, Iran, using a coupled SWAT-MODFLOW model. *Environmental Earth Sciences*, *78*, 201.

Shaw, D. A., van der Kamp, G., Conly, F. M., Pietroniro, A., & Martz, L. (2012). The fill-and-spill hydrology of prairie wetland complexes during drought and deluge. *Hydrological Processes*, *26*, 3147–3156.

Shaw, D. A., Pietroniro, A. L., & Martz, L. W. (2013). Topographic analysis for the prairie pothole region of Western Canada. *Hydrological Processes*, *27*, 3105–3114.

Smith, A. J., & Townley, L. R. (2002). Influence of regional setting on the interaction between shallow lakes and aquifers. *Water Resources Research*, *38*, 10-1-10-13.

Stumpp, C., & Hendry, M. J. (2012). Spatial and temporal dynamics of water flow and solute transport in a heterogeneous glacial till: The application of high-resolution profiles of delta O-18 and delta H-2 in pore waters. *Journal of Hydrology*, *438*, 203–214.

Sun, G., Callahan, T. J., Pyzoha, J. E., & Trettin, C. C. (2006). Modeling the climatic and subsurface stratigraphy controls on the hydrology of a Carolina bay wetland in South Carolina, USA. *Wetlands*, *26*, 567–580.

Therrien, R., Mclaren, R., Sudicky, E., & Panday, S. (2010). *A three-dimensional numerical model describing fully-integrated subsurface and surface flow and solute transport*. User Guide.

Townley, L. R., & Davidson, M. R. (1988). Definition of a capture zone for shallow water table lakes. *Journal of Hydrology*, *104*, 53–76.

Townley, L. R., & Trefry, M. G. (2000). Surface water-groundwater interaction near shallow circular lakes: Flow geometry in three dimensions. *Water Resources Research*, *36*, 935–948.

van Genuchten, M. T. (1980). A close form equation for predicting the hydraulic conductivity of unsaturated soils. *Soil Science Society of America Journal*, *44*, 892–898.

Verch, G. (2014). *Weather data 1992, Dedelow*. ZALF Open Research Data.

Vyse, S. A., Semiromi, T. A. I. E., Lischeid, G., & Merz, C. (2020). Characterizing hydrological processes within kettle holes using stable water isotopes in the Uckermark of northern Brandenburg. *Germany. Hydrol Process*, *34*(8), 1868–1887.

Winter, T. C. (1976). *Numerical simulation analysis of the interaction of lakes and ground water*. US Government Printing Office.

Winter, T. C. (1983). The interaction of lakes with variably saturated porous media. *Water Resources Research*, *19*, 1203–1218.

Winter, T. C. (1999). Relation of streams, lakes, and wetlands to groundwater flow systems. *Hydrogeology Journal*, *7*, 28–45.

Winter, T. C. (2001). Ground water and surface water: The linkage tightens, but challenges remain. *Hydrological Processes*, *15*, 3605–3606.

Winter, T. C., Rosenberry, D. O., & Labaugh, J. W. (2003). Where does the ground water in small watersheds come from? *Groundwater*, *41*, 989–1000.

Xu, S., & Ma, T. (2011). Evapotranspiration observation and data analysis in reed swamp wetlands. *IAHS Publication*, *344*, 239–244.

Zheng, C., Wang, H. F., Anderson, M. P., & Bradbury, K. R. (1988). Analysis of interceptor ditches for control of groundwater pollution. *Journal of Hydrology*, *98*, 67–81.

How to cite this article: Steidl, J., Gliege, S., Semiromi, M. T., & Lischeid, G. (2023). Groundwater flow reversal between small water bodies and their adjoining aquifers: A numerical experiment. *Hydrological Processes*, *37*(5), e14890. https://doi.org/10.1002/hyp.14890